Metadata of the chapter that will be visualized in SpringerLink

Book Title	Estuaries and Coastal Zones in Times of Global Change
Series Title	
Chapter Title	Synergy Between Hyperspectral (HYSPEX), Multispectral (SPOT 6/7, Sentinel-2) Remotely Sensed Data and LiDAR Data for Mapping the Authie Estuarie (France)
Copyright Year	2020
Copyright HolderName	Springer Nature Singapore Pte Ltd.

Corresponding Author	Family Name	**Verpoorter**
	Particle	
	Given Name	**Charles**
	Prefix	
	Suffix	
	Role	
	Division	LOG, Laboratoire D'Océanologie et de Géosciences
	Organization	Univ. Littoral Côte D'Opale, Univ. Lille, CNRS, UMR 8187
	Address	62930, Wimereux, France
	Email	charles.verpoorter@univ-littoral.fr
Author	Family Name	**Menuge**
	Particle	
	Given Name	**Benoit**
	Prefix	
	Suffix	
	Role	
	Division	LOG, Laboratoire D'Océanologie et de Géosciences
	Organization	Univ. Littoral Côte D'Opale, Univ. Lille, CNRS, UMR 8187
	Address	62930, Wimereux, France
	Email	
Author	Family Name	**Launeau**
	Particle	
	Given Name	**Patrick**
	Prefix	
	Suffix	
	Role	
	Division	
	Organization	Université de Nantes, EA 2160 MMS, Laboratoire Mer Molécule Santé de Nantes, 2 Chemin de La Houssinière
	Address	44322, Nantes, France
	Email	
Author	Family Name	**Méléder**
	Particle	
	Given Name	**Vona**
	Prefix	

	Suffix	
	Role	
	Division	
	Organization	Géodunes
	Address	19 Rue Maurice Ravel, 59240, Dunkirk, France
	Email	
Author	Family Name	**Héquette**
	Particle	
	Given Name	**Arnaud**
	Prefix	
	Suffix	
	Role	
	Division	LOG, Laboratoire D'Océanologie et de Géosciences
	Organization	Univ. Littoral Côte D'Opale, Univ. Lille, CNRS, UMR 8187
	Address	62930, Wimereux, France
	Email	
Author	Family Name	**Cartier**
	Particle	
	Given Name	**A.**
	Prefix	
	Suffix	
	Role	
	Division	LOG, Laboratoire D'Océanologie et de Géosciences
	Organization	Univ. Littoral Côte D'Opale, Univ. Lille, CNRS, UMR 8187
	Address	62930, Wimereux, France
	Division	
	Organization	Université de Nantes, UMR 6112 CNRS, Laboratoire de Planétologie et Géodynamique de Nantes, 2 Chemin de La Houssinière
	Address	BP 92208, 44322, Nantes, France
	Division	
	Organization	Université de Nantes, EA 2160 MMS, Laboratoire Mer Molécule Santé de Nantes, 2 Chemin de La Houssinière
	Address	44322, Nantes, France
	Division	
	Organization	Géodunes
	Address	19 Rue Maurice Ravel, 59240, Dunkirk, France
	Email	
Author	Family Name	**Sipka**
	Particle	
	Given Name	**Vincent**
	Prefix	
	Suffix	
	Role	
	Division	LOG, Laboratoire D'Océanologie et de Géosciences
	Organization	Univ. Littoral Côte D'Opale, Univ. Lille, CNRS, UMR 8187
	Address	62930, Wimereux, France

	Email
Abstract	The Authie estuarie, located at the eastern part of the English Channel is of environmental, ecological, economic and societal importance. With the intention to better understand the sediment dynamic it is important to better assess the role of sediment dynamics including erosion, stabilization and sediment reworking processes which is challenging in such complex environment. It is also important to consider biogenic components such as the microphytobenthos (MPB) distribution, as the primary productivity may play an important role with the bio-stabilization process. As a consequence, there is a crucial need to provide a synoptic overview of inherent bio-physical characteristics of sediments (i.e., composition, water content, grain-size, and biomass) in estuarine environment by generating precise quantitative maps for predicting in a second step estuarine evolution by including sediment transport, sedimentation rates, coastal flows processes and sea level rise caused by climate change for instance. The use of the remote sensing technology is increasingly used for mapping estuarine and coastal environments by providing a synoptic overview of bio-physical characteristics of sediments. In that sense, the combination between remote sensing imaging, topographic data (LiDAR) and *in situ* measurements is suitable for improving our understanding of sediment dynamics with respect to physical and biological forcings. The main objective of this study is to demonstrate that the synergy between multispectral (i.e., SPOT 6–7 [1.5 m/pixel]; Sentinel-2, 10–60 m/pixel, 5–10 days)", hyperspectral [Hyspex, 70 cm/pixel, 160 spectral bands] remote sensing images may be suitable for generating both reliable sedimentary and primary productivity budgets; at least for surficial sediments. All presented data were acquired during the same day (09/21/2017) in the framework TéléEST, CPER MARCO and CNRS-OMPBI projects.
Keywords (separated by '-')	Remote sensing - Hyperspectral - Multispectral - LiDAR - Physical properties mapping - Morphology - Bay of authie

Synergy Between Hyperspectral (HYSPEX), Multispectral (SPOT 6/7, Sentinel-2) Remotely Sensed Data and LiDAR Data for Mapping the Authie Estuarie (France)

Charles Verpoorter, Benoit Menuge, Patrick Launeau, Vona Méléder, Arnaud Héquette, A. Cartier and Vincent Sipka

Abstract The Authie estuarie, located at the eastern part of the English Channel is of environmental, ecological, economic and societal importance. With the intention to better understand the sediment dynamic it is important to better assess the role of sediment dynamics including erosion, stabilization and sediment reworking processes which is challenging in such complex environment. It is also important to consider biogenic components such as the microphytobenthos (MPB) distribution, as the primary productivity may play an important role with the bio-stabilization process. As a consequence, there is a crucial need to provide a synoptic overview of inherent bio-physical characteristics of sediments (i.e., composition, water content, grain-size, and biomass) in estuarine environment by generating precise quantitative maps for predicting in a second step estuarine evolution by including sediment transport, sedimentation rates, coastal flows processes and sea level rise caused by climate change for instance. The use of the remote sensing technology is increasingly used for mapping estuarine and coastal environments by providing a synoptic overview of bio-physical characteristics of sediments. In that sense, the combination between remote sensing imaging, topographic data (LiDAR) and *in situ* measurements is suitable for improving our understanding of sediment dynamics with respect to physical and biological forcings. The main objective of this study is to demonstrate

C. Verpoorter (✉) · B. Menuge · A. Héquette · A. Cartier · V. Sipka
LOG, Laboratoire D'Océanologie et de Géosciences, Univ. Littoral Côte D'Opale, Univ. Lille, CNRS, UMR 8187, 62930 Wimereux, France
e-mail: charles.verpoorter@univ-littoral.fr

A. Cartier
Université de Nantes, UMR 6112 CNRS, Laboratoire de Planétologie et Géodynamique de Nantes, 2 Chemin de La Houssinière, BP 92208, 44322 Nantes, France

P. Launeau · A. Cartier
Université de Nantes, EA
2160 MMS, Laboratoire Mer Molécule Santé de Nantes, 2 Chemin de La Houssinière, 44322 Nantes, France

V. Méléder · A. Cartier
Géodunes, 19 Rue Maurice Ravel, 59240 Dunkirk, France

K. D. Nguyen et al. (eds.), *Estuaries and Coastal Zones in Times of Global Change*, Springer Water,
https://doi.org/10.1007/978-981-15-2081-5_45

that the synergy between multispectral (i.e., SPOT 6–7 [1.5 m/pixel]; Sentinel-2, 10–60 m/pixel, 5–10 days)", hyperspectral [Hyspex, 70 cm/pixel, 160 spectral bands] remote sensing images may be suitable for generating both reliable sedimentary and primary productivity budgets; at least for surficial sediments. All presented data were acquired during the same day (09/21/2017) in the framework TéléEST, CPER MARCO and CNRS-OMPBI projects.

AQ1

Keywords Remote sensing · Hyperspectral · Multispectral · LiDAR · Physical properties mapping · Morphology · Bay of authie

1 Introduction

With the intention to improve our understanding of sediment dynamics within estuarine environments such as the Bay of Authie (North of France) it is crucial to generate precise quantitative maps of physical and biological properties of the sediment deposits. Inherent sedimentary parameters such as grain-size, moisture content, biological content, topography as well as physical forcing conditions (e.g. tidal conditions and wave currents) are needed for retrieving environmental changes over time and therefore to be able to generate reliable sedimentary budgets prior to define any management strategies or any decisions which may help to overcome erosion or sandfilling issues. Sedimentary trend predictions are generally based on field data such as samples sediments, in situ measurements but also any precise quantitative maps. In that sense remotely sensed products, maps of sedimentary parameters, may be assimilated by models such as transport models, erosion/stabilization models and thus for computing those predictions under various scenario. Even hydrodynamic condition knowledge is needed for fully assessing the general sedimentary trend, in this study, we decided to only focus on inherent sedimentary parameters mapping. Grain-size maps are important for fully assessing sediment transport trend, erodibility of sediment surfaces, etc. It is also important to consider moisture content both in sedimentology aspects as it influences the cohesiveness behavior of sediments and in ecology aspects for mapping habitats or evaluating hydration stress conditions for example. Microphytobenthos (MPB), a photosynthetic benthic microalga, is in partly responsible of the bio-stabilization process. Consequently, mapping of MPB biomass is important for fully assessing the reworking sediment processes.

Remote Sensing is now considered as an useful tool for mapping physical properties of sediments (Rainey et al. 2003; Deronde et al. 2008; Adam et al. 2010; Small et al. 2009; Verpoorter et al. 2014) or biophysical properties (Combe et al. 2005; Méléder et al. 2010; Launeau et al. 2018). While remote sensing tool presents the advantage to get a synoptic overview of coastal zones with wide swaths, scenes analyzed for mapping are only restricted to few millimeters of sediment surfaces limiting our understanding of sedimentary processes over time to approximately one or several tidal cycles. Nevertheless several processes such as erosion, stabilization, bio-stabilization, transport and deposition can be assessed over time using imagery

Table 1 Spatial and spectral resolutions of sensors used

Hyspex 1600 VNIR		SPOT 6/7		S2	
Spatial resolution (m/pixel)	Spectral bands	Spatial resolution (m/pixel)	Spectral bands (nm)	Spatial resolution (m/pixel)	Spectral bands (nm)
0.7	160 bands between 400 and 1000 nm	6	450–520	10	425–555
			530–590		525–595
			625–695		635–695
			760–890		
		1.5	450–745		727–957

at high spatial resolution (SPOT 6/7, 1.5 m/pixel; Sentinel-2 (S2), ~10 m/pixel). The high spatial SPOT 6/7 multispectral satellite is well designed for that purpose. Although SPOT 6/7 multispectral data enable us to precisely map sedimentary and geomorphic structures (e.g, ridges and runnels, mega-ripples, spit, waterline, shoreline, etc.) at various scales of observation, S2 sensor presents the benefit to have a very high repetitive time over the same scene (3–5 days with the S2A and S2B configuration) allowing to generate homogenous time-series. Multispectral data contain few spectral channels (Table 1) compared to hyperspectral data. When spatial resolution of hyperspectral sensors which are generally mounted onboard an aircraft are maximized, hyperspectral images are well-suited for deriving accurate quantitative maps with respect to spectral models used. It is explain by the fact that hyperspectral sensor is the only one allowing the collection of a contiguous reflectance spectrum per pixel in numerous narrow spectral bands. In this study, we proposed to use the synergy between various optical sensors operated onboard satellites (SPOT 6/7 and S2) and airborne platforms (HySpex 1600 VNIR) for mapping sedimentary parameters variability at low tide and thus during the same day (09-21-2016).

The main objective of this study consists in 1) mapping sediment properties by tacking the advantage of the synergy between remotely sensed data (SPOT 6/7, S2, and hyperspectral image termed HySpex) and LiDAR data. Bedform dynamics will be examined by calculating topography changes with two sets of LiDAR data between 2013 and 2016.

2 Study Site

The Authie estuary (50° 22′ 25″ N, 1° 37′ 52″ E, Fig. 1a is located on the French coast of the Eastern English Channel (EEC), and it is characterized by a semi-diurnal and macrotidal regime. The Authie estuary is a "picard" type-estuary according to the Briquet et al. (1930) study. The Authie estuary forms a shallow elongated embayment oriented SE/NW (N120). It is affected by a general sandfilling and it presents a typical geomorphology structures, in accretion to the south zone such as 'la pointe

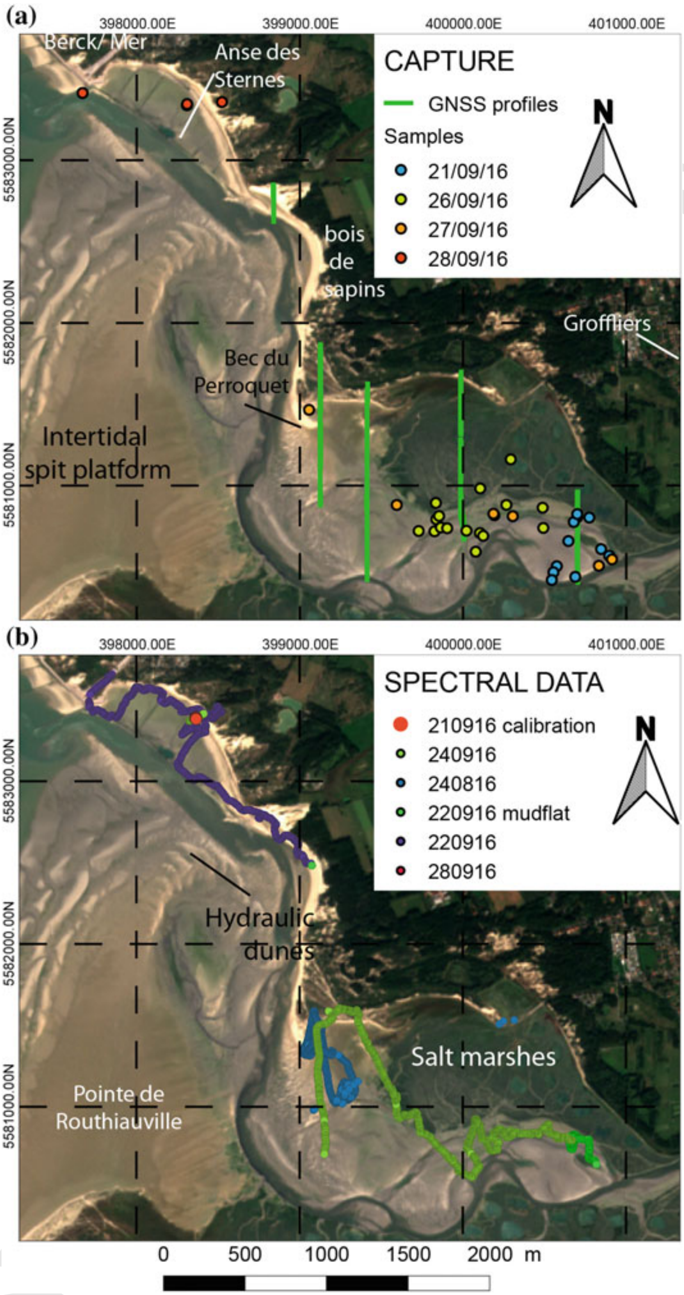

Fig. 1 In situ investigations in the Authie Bay. **a** Sediment samples and GNSS cross-shore profiles, **b** radiometric measurements acquired between the 21th of September 2016 and the 21st of September 2016

de Routhiauville' spit which reflect a northward progradation (~6.1 m/an between 2005 and 2012; Dobroniak 2005; Sogreah 2009; Hesp et al. 2016) in contrast with the northern part which is affected by a local erosion. The Authie sea-chenal deviates to the North as a response of the spit accretion and the sandfilling. As a consequence, the northern coastal line is affected by erosion of the secondary sediment cells such as 'la Grande dune' (sand-dune), 'Bois de Sapins' (pine forest) and the 'Anse des Sternes' (a well-protected area) with an erosion rate of 50.000 m^3/an (Sogreah 2009). All reworked sand sediments participate to the general infilling of the inner bay. In the medium estuary, a secondary spit structure (a cuspate foreland) was in accretion, termed the 'Beck du Perroquet' testifies to this sandy transport until the salt-marches. It is a southward prograding system (Hesp et al. 2016). The sediment coverage is highly controlled by the tidal conditions with a general decrease in particle-size from the marine estuary to the low estuary. Along the marine side, the morphology is marked by the presence of ridges and runnels (sedimentary bars) which is a particular characteristic of the EEC macrotidal coastal system. It is composed by coarse to medium sizes of sand-deposits. Upper and middle part of the estuary are mainly composed by intertidal sand flats and sandy bars ranging from fine sizes (D50 = 0.1 mm) to medium sizes (D50 = 0.6 mm) including a shelly debris component. Low estuary is mainly composed by silty sediments. Mudflats and salt-marches occur mainly in the inner estuary (Deloffre et al. 2007) as well as in the Anse des Sternes as these zones are relatively well-protected from wave-current by breakwater and groynes. Whatever the sites considered MPB, mainly diatoms, can form biofilm patches on muddy sediments. Due to the described overall sandy-transport pattern, it is not rare that during a tidal cycle some sand sediment might recover the existing muddy surfaces within the salt marshes and mudflats.

3 Materials and Methods

As mentioned before, here it is proposed to map sediment parameters by integrating the synergy between a MultiSpectral Instrument (MSI) on Sentinel-2 (S2) platform, a high spatial resolution image (SPOT 6/7), high spectral resolution images called hyperspectral images (HySpex) and LiDAR topographic data. In the framework of the 'Défi littoral OMPBI' project the Authie Bay was imaged on September 21th 2016 between 9:07 and 09:58 (UTC) by a hyperspectral/LiDAR campaign at low tide.

Sediments samples (Fig. 1a) and cross-shore elevation profiles were also collected using a GNSS (Leica TPS Syst1200) with vertical and horizontal accuracy of ±2.5 cm and ±1.5 cm respectively (Fig. 1a, in green line) at the same day for further assessments and validations. Radiometric measurements were also performed using an ASD Fieldspec 4 FR4 [2500 spectral bands]) in order to calibrate hyperspectral images and also have a reliable atmospheric correction (Fig. 1b, red spot). The in situ survey was conducted during one week, where further samples and radiometric data were collected (Fig. 1). A total of 65 surficial sediment samples were collected across

Fig. 2 Tidal condition and airborne-satellites overpass configuration in 21st of September 2016

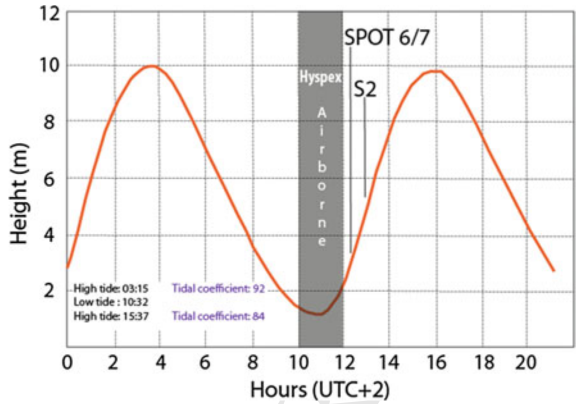

the intertidal and supratidal domains during one week and at low tide (Fig. 1a). Conditions for further investigation in grain-size, chlorophyll-a concentration (10 samples).

In situ and laboratory dataset were used for validation of spectral models. Then sediment samples were analyzed under laboratory conditions. Chlorophyll-a contents were measured using a spectrophotometer on a set of 10 samples acquired during the overflight. Grain-sizes analyses were performed using LS230 laser particle-sizer (© Beckman Coulter). Grain size parameters (mean, sorting and skewness), sedimentary facies and classes were calculated using the GRADISTAT software (Blott and Pye 2001) following the Folk and Ward (1957) methods.

Multispectral remotely sensed data (SPOT 6/7 and S2) were acquired more or less 30–60 min after the airborne overpass (Fig. 2). While LiDAR data were acquired simultaneously with the hyperspectral images (HySpex'sensor) we can assume that topography and main geomorphic structures did not affected by significant changes from an image to another one, at least in the inner estuary. Such as multi-sensors configuration is judged to be really rare and it offers us the opportunity to map sedimentary facies under topographic controlled during the immersion time.

SPOT6/7 image was ordered in the frame of the GEOSUD program. Initially the multispectral bands (6 m/pixel) were pan-sharpened to the panchromatic one (1.5 m/pixel) for enhancing the spatial resolution of all spectral bands to 1.5 m/pixel using the Gram –Schmidt pan-sharpening technique (Laben and Bower 2000). Then, raw images were calibrated and corrected from atmospheric effects using the FLAASH method. With a spatial resolution of 1.5 m/pixel (Table 1), the spatial resolution is sufficient to discriminate accurately sedimentary structures of bedforms such as sedimentary bars, mega-ripples, creeks, sea-channel, etc.

Sentinel-2 sensor was operated belong ESA (European Spatial Agency) and delivered throughout the THEIA platform into a L2A format following the MAJA method (Hagolle et al. 2010). MAJA is an evolution of MACCS (Multi-sensor Atmospheric Correction and Cloud Screening), in which a couple of methods inspired by ATCOR

483190_1_En_45_Chapter ✓ TYPESET DISK LE ✓ CP Disp.:12/12/2019 Pages: 21 Layout: T1-Standard

software have been added. With a spatial resolution of 10–20 m per pixel, the resolution is not sufficient to discriminate accurately all sedimentary structures at fine-scale such as some of the mega-ripples. However, S2 is well-suite for mapping meso-scale structures such as sandy spit, main channel, ridges and runnels, some of the mega-ripples, etc.

Hyperspectral images were acquired with a HySpex Visible Near InfraRed (VNIR) 1600 camera having a spectral resolution of 4.5 nm in 160 spectral channels between 400 and 1000 nm. Simultaneously, topographic data were acquired with the LiDAR platform of Nantes-Rennes universities with a spatial resolution of 1 m/pixel. Fly conditions was set-up for maximizing the spatial resolution of hyperspectral data at 0.7 m per pixel. Atmosphere correction was performed with the ATCOR 4/ MODTRAN. A Minimum Noise Fraction (MNF) transformation (Green et al. 1988) was applied to images to reduce noise from signal.

A digital terrain model (DTM) was generated with a spatial resolution of 1 m per pixel (Fig. 3). In addition, GNSS data (2273 ground control points) were used for minimizing error in areas covered dense vegetation. DTM correction was performed based on a linear regression approach between LiDAR data and GNSS ground control

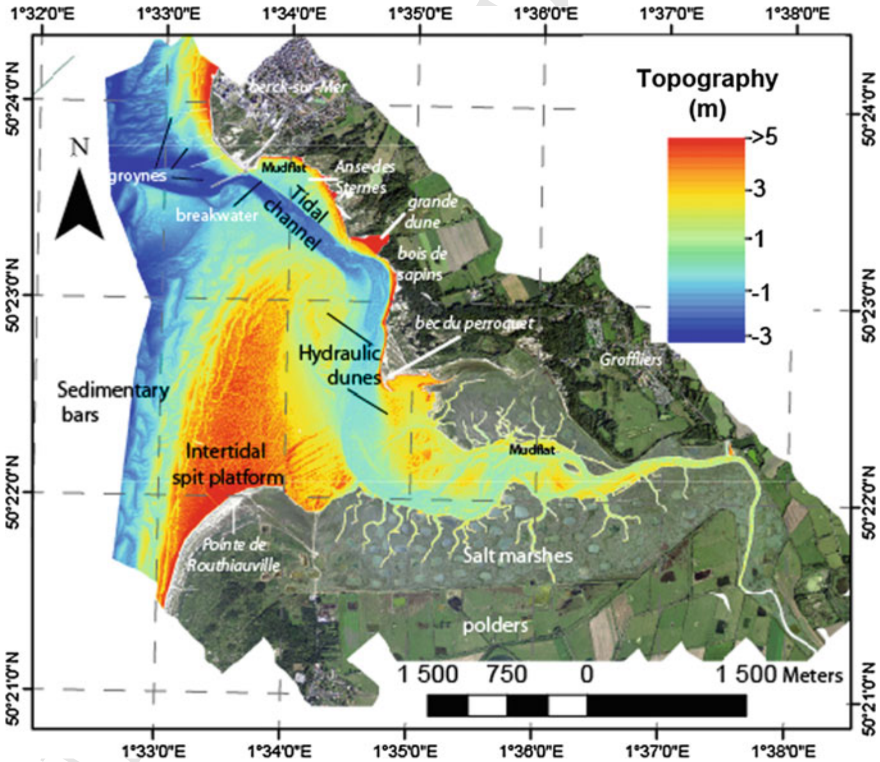

Fig. 3 Morphology map of the Authie estuary generated from LiDAR data, 21st of September 2016

points (y = 1.005–0.39, R^2 = 0.99, RMSE = 0.386). Figure 3 displays the bay morphology including ridge and runnels, crest of sedimentary bars, hydraulic dunes, salt marshes, etc. In addition, in the framework of the SNO DYNALIT previous a LiDAR topographic data (ALS60 LiDAR, © Leica Geosystems) was acquired in December 2013 by the Circle operational teams. The planimetric position accuracy of the data points range from ±0.10 to 0.17 m with a vertical accuracy b ± 0.10 m as verified by several ground control points. In this study we only compare the 2016 LiDAR data to the 2013 one. Topographic discrepancies were computed for interpreting the morpho-sedimentary dynamics and characteristics of the sea-bed estuary.

With the intention to derive maps of sediment parameters, several spectral models were used according to the spectral resolution. When mapped with multispectral sensors, biomass is usually expressed in NDVI (Normalizes Differential Vegetation Index, Tucker 1979) values. Another spectral index called MPBI index was proposed by Méléder et al. (2010) to distinguish MPB from macrophytes. In this study, two methods were tested. Combe et al. (2005) developed a non-linear unmixing model for hyperspectral data based on MGM (Modified Gaussian Model) continuum removal. Even if this model is recognized to be well-appropriate for very high spectral resolution data, we tested a similar approach designed for multispectral data. Basically the developed approach stills the same except that we didn't perform any continuum removal prior to derive biomass and it is based on a linear unmixing approach. For simplicity, this method was called LMM for Linear Mixing Method. Compared to spectral indices methods, LMM has the advantage to integrate sandy and muddy surfaces into the mixing itself.

However, when mapped with hyperspectral resolution, advanced spectral model may be used allowing to analyze the full shape of continuous reflectance spectra and narrow absorption bands characteristics with respect to different MPB groups (Combe et al. 2005). In the framework of the OMPBI project, a radiative transfer algorithm called MPBOM (MicroPhytobenthos Optical Model) was applied with hyperspectral data (Launeau et al. 2018). While many biomass products could derived from this model, here the latter was only used to retrieve the biofilm absorption coefficient α which was linearly related to biomasses. Then, MPBOM outputs were briefly compared to the unmixing algorithm outputs.

With the intention to compare maps of grain-size and water content parameters for each of sensors used, we decided to apply a simple multispectral algorithm (see *more detailed in appendices*) based on spectral features and in situ measurements of collocated sediment surfaces. Basically, algorithms consisted in confronting in situ measurement (mean grain-size) to reflectance value of the images. For such as comparison, hyperspectral images were resampled to the SPOT 6/7 spectral resolution.

483190_1_En_45_Chapter ✓ TYPESET ☐ DISK ☐ LE ✓ CP Disp.:12/12/2019 Pages: 21 Layout: T1-Standard

4 Results

4.1 Morphology of the Seabed

Surface elevation evolution can be retrieve using LiDAR data acquired at different periods. Topographic differences enable us to quantify precisely the relative sedimentary budget trend. Crapoulet (2015) calculated a positive budget for the overall Authie estuary from LiDAR data acquired between 2008 and 2011 about 827,162 m^3 (+0.08 m^3/m^2). Conversely, they calculated a negative budget for the overall Authie estuary from LiDAR data acquired between 2011 and 2013 about −569,529 m^3 (−0.05 m^3/m^2). As a consequence, between 2008 and 2013 there is a volumetric gain of +111,191 m^3 (+0.01 m^3/m^2).

We propose here to revise the budget number by integrating new LiDAR data acquired during the OMPBI survey from 2013 to 2016. Basically DTMs relative map differences were computed exhibiting a sea-bed dynamics allowing to identify erosion (blue-yellow-orange) and accretion (in red) zones. The relative sedimentary budget remains negative over the overall estuary (Mean = -0.41 ± 0.859 m^3/m^2) which is consistent with Crapoulet (2015) study. Indeed, a negative budget for the overall Authie estuary from LiDAR data acquired between 2011 and 2013 about −219,239 m^3 (−0.04 m^3/m^2). As a consequence, between 2008 and 2016 there is a volumetric loss of −108,048 m^3 (−0.02 m^3/m^2). Consequently the net changes in elevation surface between 2008 and 2016 reveals a significant loss of volume on the overall estuary.

Because ridge and runnels (sedimentary bars) and mega-ripples systems are highly dynamics from a tidal cycle to another one, they are not representative of the sedimentary budget for such a long period ~3 years. Intentionally we do not consider them into our sedimentary budget and we restricted our calculations to several representative zones within the inner estuary (‘Bois de Sapins’, mudflats, ‘Anse des Sternes’, ‘Bec du Perroquet’, middle estuary and spit platform).

Observations (Fig. 4) are consistent with literature as the ‘Bois de Sapins’ is affected by strong erosion (blue color) with a decrease of elevation ranging from −9 to 3 m (Mean = -1.2 ± 1.3 m^3/m^2). This is explains by the fact that the estuary mouth is largely blocked by the prominent sand spit platform, and this has forced the Authie channel of the estuary to flow along the northern shore. As the consequence, this zone concentrates a maximum of energy. Despite that the anthropic area called ‘Anse des Sternes’ is well protected from waves and currents with breakwater and groynes structures, the sedimentary budget is slightly negative with an elevation ranging from −6 to 0.8 m (Mean = -0.5 ± 0.2 m^3/m^2). The eastern part of the ‘Bec du Perroquet’ presents slight negative elevation variations with an elevation surface ranging from −2.3 to 1.5 m (Mean = -0.23 ± 0.27 m^3/m^2). Natural mudflats located along the northern salt-marches are affected by a slight erosion (yellow color) with a decrease of elevation ranging from −2 to 0.65 m (Mean = -0.3 ± 0.3 m^3/m^2). The spit platform budget is slightly negative with an elevation ranging from −1.6 to 1.0 m (Mean = -0.41 ± 0.01 m^3/m^2). Negative budgets observed in mudflats, spit and

483190_1_En_45_Chapter ☑ TYPESET ☐ DISK ☐ LE ☑ CP Disp.:12/12/2019 Pages: 21 Layout: T1-Standard

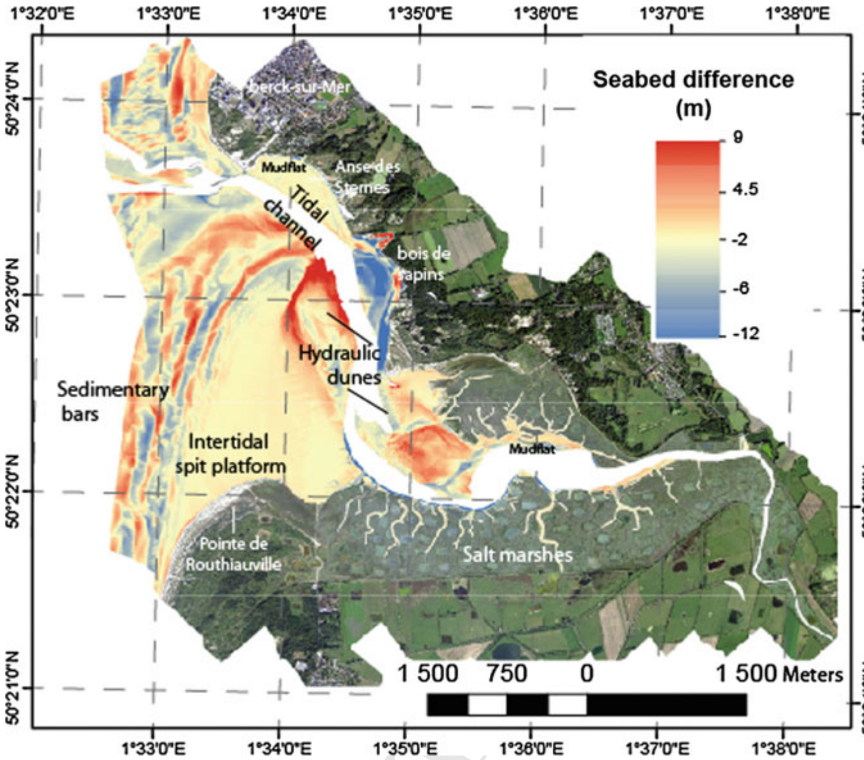

Fig. 4 Net changes in surface elevation between December 2013 and September 2016 based on LiDAR topographic data

anywhere else can be explained by the fact that the sediment supply may decrease over time explaining that there is less deposits or that the sediment compaction processes might more efficient.

While the overall estuary presents a negative budget, several zones are clearly affected by accretion such as the middle estuary and the north of the backside part of the spit. In the middle estuary, there is a positive elevation (in red) variation ranging from −1.3 to 1.3 m (Mean = 0.25 ± 0.30 m^3/m^2). This positive budget can be explained by the fact that the allochthonous sediments coming from the maritime side and autochthonous sediments coming from erosive sites may increase over time due to high sedimentary transit during the flood-tide and thus until their deposits. To conclude some sediment accumulations occurred downdrift to the south, but only took place at middle estuary. The backside of the spit platform budget presents a positive budget (in red) mainly in the northern part with an elevation ranging from −0.83 to 2.8 m (Mean = 1.0 ± 0.6 m^3/m^2). This may be explained by the fact that the spit is prograding toward the N–W part of the bay. In addition, reworking sediments coming from the erosion sites may contribute of some sediment accumulations downdrift to the south, but only took place at tip of northern spit.

Finally, regarding the supratidal domain, ‘la Grande Dune’, a parabolic dune seems to be in accretion at the top due to Aeolian deflation inputs which may coming from intertidal sandy bars, generally drier than the rest of intertidal sediments. The bottom part of this dune is in erosion. With a ranging from −10 to 9 m (Mean = −0.65 ± 2.40 m^3/m^2) the overall budget is slightly negative.

4.2 MPB Spatial Distribution Mapping

As mentioned before a LMM spectral model was applied at multispectral resolution sensors allowing to compare biomass output products together (Fig. 5). Whatever the sensor used MPB generally occurs over fine sediment substrates such as very fine-sands or silts. High MPB concentrations are mainly present on mudflat sediments (‘Anse des Sternes’ and along salt-marshes). In details, MPB was locally observed at the bottom of mega-ripples with respect to the spatial resolution of the sensors. This is explained by the fact that grain-size may slightly decrease and that moisture content is generally higher compare to mega-ripple crests. Surprisingly, MPB also occurs on most part of the spit. Despite that the spit structure is mainly composed by sandy sediments (135 ± 40 µm; HySpex), it is possible to observed a very thin layer composed by muddy sediment covering the sand substrates. This might appear when tide energy becomes lower during low tide. However, it is well-known that MPB distributions are not only a function of the sediment cover-type (sand or mud), it may also vary in time and space as a function of numerous factors like: time of emersion, solar energy, and nutrients inputs, etc. Because images were acquired at various times of acquisitions at the same day, sensors synergy offers us a unique opportunity for mapping the evolution of the MPB distribution during a tidal cycle especially at the emersion time. Figure 5 exhibits strong spatial variation in biomass concentrations which means that MPB migration is highly dynamic at short time during aerial exposure. It seems that the MPB concentration spatially decrease from 10:00 to 13:00 UTC+2 which means that the maximum of MPB production is observed with a mean value of 27 ± 19 $mg.m^{-2}$ during the HySpex overpass (Fig. 5a) while the minimum of MPB production (Fig. 5b) is observe during the S2 overpass (Fig. 5c) with a mean value of 17 ± 13 mg m^{-2}. Intermediate values are observed during the SPOT 6/7 overpass (Fig. 5b) with a mean value of 21 ± 18 mg m^{-2}. Note that the MPB variability was correlated to the PAR (Photosynthetically Active Radiation) values. Although these general patterns reveal a decrease in biomass coverages, in details some patches do not follow this trend. Clearly the S2 image reveals some patches with higher chlorophyll-a content than the SPOT6/7 or HySpex ones.

Although MPB production seems to be correlate to the solar radiation changes as a first order, other parameters may have a significant influence on it. Indeed, it is known that MPB migration may be influenced by the tidal range. For example, we denote that during the S2 overpass, the flood-tide coming back in the western part of the upper estuary, as a consequence it may induce an impact in our estimates. On the other hand, spatial resolution may also have a significant impact on MPB estimates due to

483190_1_En_45_Chapter ☑ TYPESET ☐ DISK ☐ LE ☑ CP Disp.:12/12/2019 Pages: 21 Layout: T1-Standard

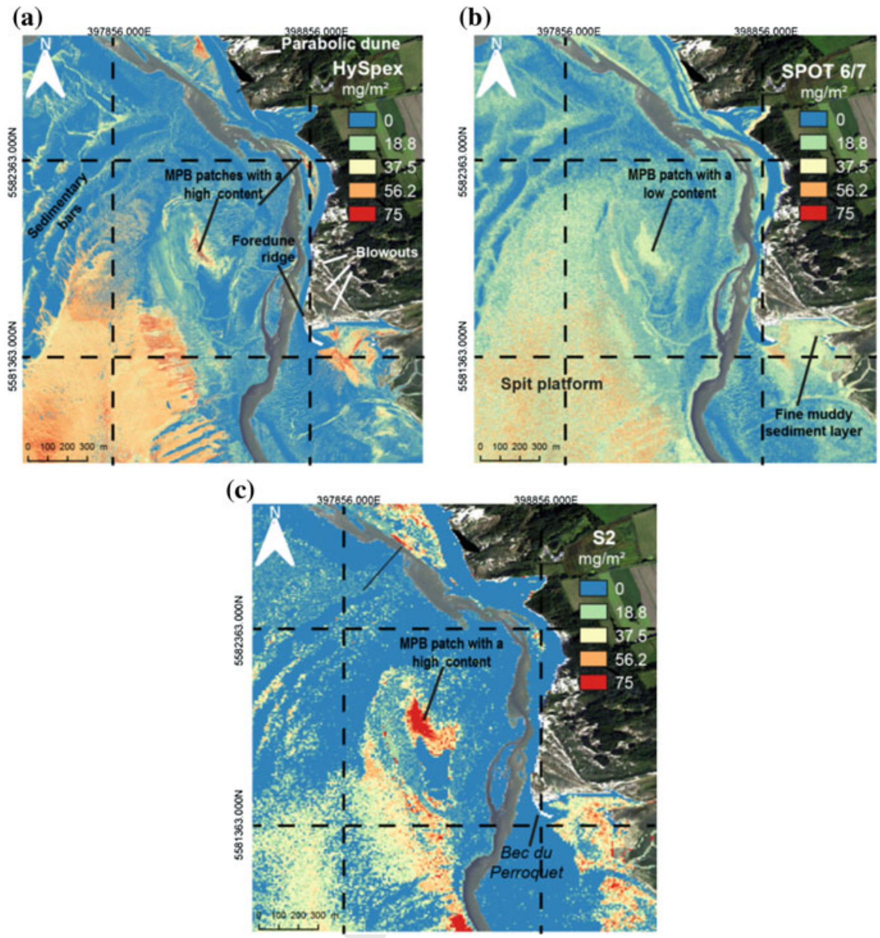

Fig. 5 Maps representing the net primary production (in mg m^{-2}) at low tide (09/21/2016) from **a** HySpex VNIR; **b** SPOT 6/7 and **c** S2 data and by applying the Liner Mixing Model (LMM)

non-linear mixing between natural surfaces within a pixel. Because, S2' resolution is coarser than SPOT 6/7 (with a factor ~3) and HySpex ones (with a factor ~14), the probability that MPB covers are mixed with abiotic surfaces (e.g. sand or mud) is pretty high. As a result, biomasses may be underestimated. It is one of the reasons why more advanced methods such as non-linear unmixing model (Combe et al. 2005) or none-scale dependent approaches such as the MPBOM (Kazemipour et al. 2012) still desirables. However, those methods cannot be applied on multispectral data.

MPBOM was applied to hyperspectral HySpex images in the framework of the 'Défi littoral OMPBI' project. Among biomass products (coefficient of absorption, peak of the Chl-a, biomass of the MPB) the distribution of the absoption coefficient peak at 673 nm was analyzed. Figure 6 display the total chlorophyll-a distribution

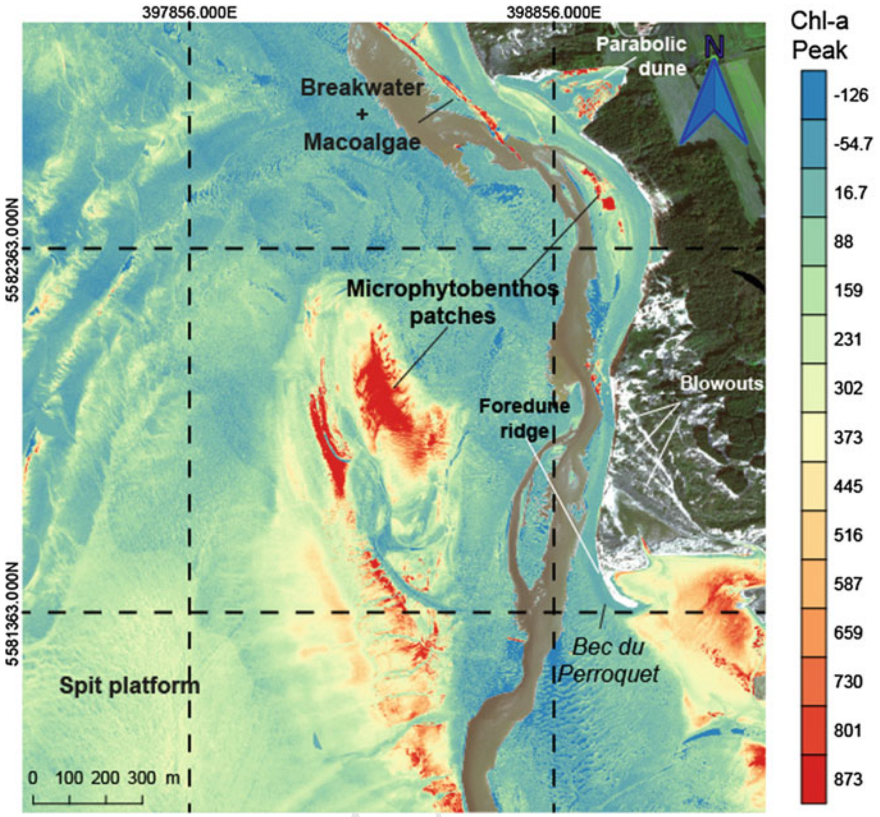

Fig. 6 Map representing the peak of the absorption coefficient at 673 nm during low tide (09/21/2016) from HySpex VNIR data and by applying the MPBOM in the framework of the 'Défi littoral OMPBI' project

deriving from the absoption coefficient peak at 673 nm. High absorption contents are observed on the breakwater. High chlorophyll contents composed by microphytobenthos are generally observed in the backside of the spit platform and muddy sites. As mentioned before, during the airborne campaign 10 samples were collected for calculating the chlorophyll-a concentration and compared them at the pixel location of the HySpex data. MPBOM pixels are positively correlated with these samples ($R^2 = 0.57$). However, for better assessment more samples are needed. MPBOM product (Fig. 6) exhibits clearly strong discrepancies with the LMM (Fig. 5a), especially over the spit whereas similar trend is observed with S2 data especially over some patches (Fig. 5c).

Because MPBOM take into account non-linear mixing effects, we can assume that non-linear effects may induce an overestimation of the biomass with multispectral models used here.

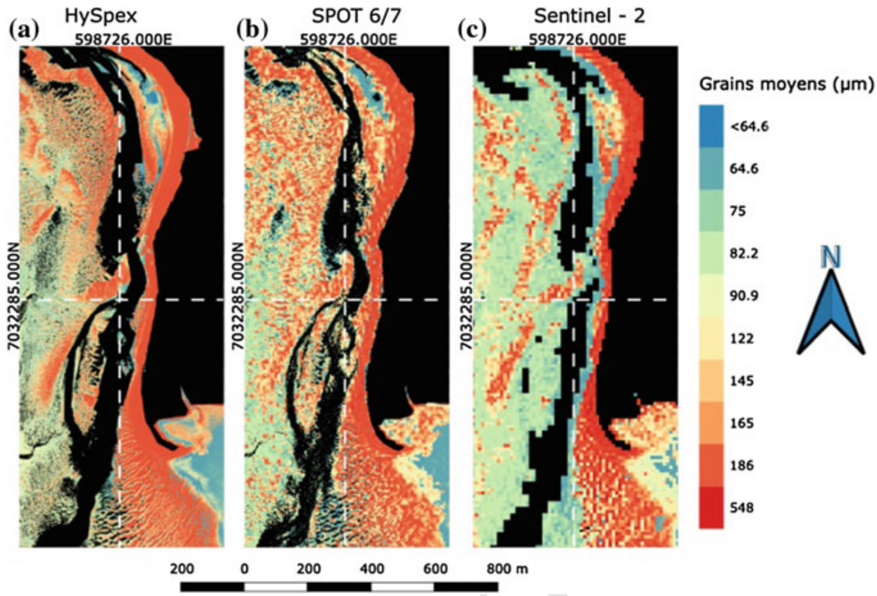

Fig. 7 Maps representing the grain-size distribution (in µm) at low tide (09/21/2016) from A) HySpex VNIR; B) SPOT 6/7 and C] S2 data and by applying experimental spectral model

4.3 Physical Properties of Surficial Sediments

As mentioned before an experimental spectral model was applied at multispectral resolution sensors allowing the comparison of physical properties (grain-size and moisture content) products together. Whatever the sensor used, grain-size (Fig. 7) and moisture content (Fig. 9) display similar patterns with a high spatial correlation.

Grain-size product validations were performed using true field data as reference. During the airborne campaign among the overall collected samples, 26 samples were analyzed using Coulter LS230 laser particle-sizer for calculating the mean grain-size and compared them at the pixel location of the satellite images. RMSE calculations ($RMSE_{HySpex} = 52\ \mu m$; $RMSE_{SPOT\ 6/7} = 40\ \mu m$ and $RMSE_{S2} = 44\ \mu m$) reveals that the range of variation between pixel values and true field data is quite low providing reasonable estimates for differencing sediment surface fraction sizes.

In Fig. 7, coarse sediments (red color) are observed on beaches, on the crest of mega-ripples, on sediment sandy bars, spit, and dunes where topography values are relative higher than the rest of the slikke (green-blue color). Locally, coarse sediments are present in shell beds deposit. The intertidal domain is mostly composed by fine sand and very fine sand sediments (~85%). Silty sediments are particularly observed on mudflat (blue color) where hydrodynamic conditions are low in energy. Mean grain-size of the Authie Bay reaches an average of 120 ± 50 µm of 170 ± 70 µm of 160 ± 70 µm at the HySpex, SPOT 6/7 and S2 resolutions. S2 image displays a large amount of fine-sediments pixels (in green) in comparison with the HySpex

483190_1_En_45_Chapter ✓ TYPESET DISK LE ✓ CP Disp.:12/12/2019 Pages: 21 Layout: T1-Standard

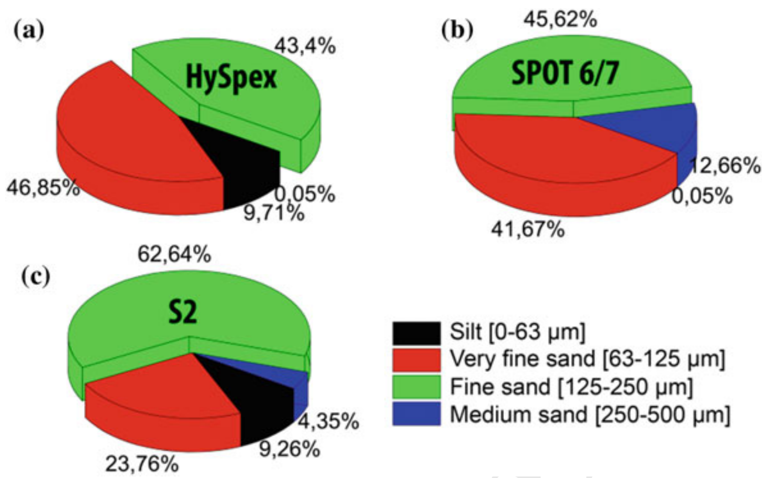

Fig. 8 Pie diagrams representing the grain-size distribution (in %) for each sensor: A) HySpex VNIR; B) SPOT 6/7 and C] S2 images

image which display coarser sediment pixels (in red). The SPOT 6/7 image displays intermediate values (in orange). With respect of the spatial resolution used, grain-size products display some major discrepancies. Indeed the coarser the spatial resolution is, the coarser the grains-size is (Fine sand + medium sand).

Whatever the sensor used (Fig. 8), fine sand sediments represent the grain-size fraction which is thee more abundant (HySpex: 43%, SPOT 6/7: 45% and S2: 62%) followed by very fine sands (HySpex: 46%, SPOT 6/7: 41% and S2: 23%) silts (HySpex: 9%, SPOT 6/7: 45% and S2: 62%) an medium sands (SPOT 6/7: 12% and S2: 9%).

Accordingly, grain-size products are impacted the spatial resolution of the sensors which might lead to an overestimate or an underestimate in the final products. Again, this explained by the non-linear unmixing effect which is not taking into account with experimental spectral model developed. Contrary to microalgae surfaces which are highly dynamic over time, grain-size fractions should not exhibit strong changes during the low tide, even slightly reworking may locally appear (e.g. grazing, feeding). As a consequence, we can assert that spectral resolutions and scale factors are respectively main factors explaining those discrepancies.

In Fig. 9, dry sediments (red color) are observed on beaches, on crests of mega-ripples, on sediment sandy bars, spit, and dunes where topography is relative higher than the rest of the slikke (green-blue color). Very moist-sediments are observed in mudflats. It is not rare to observe a thin surficial water layer over sediment substrates. Water content is widely influenced by the porosity of sedimentary structures as well as time of aerial exposure during a tidal cycle. It is clear that grain-size patterns are spatially correlated to water content patterns. This is simply explained by the fact that coarser sediments are drier than silty sediments due to the higher efficiency in the percolation process. Water content products are also influenced spectral resolutions of

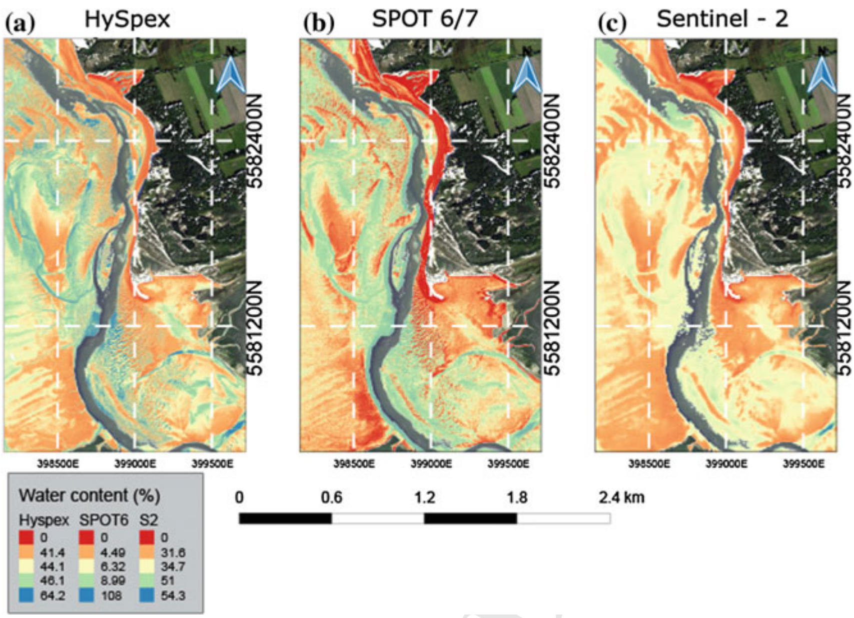

Fig. 9 Maps representing water content (in %) at low tide (09/21/2016) from **a** HySpex VNIR; **b** SPOT 6/7 and C] S2 data and by applying experimental spectral model

sensors used. Some of the S2 water-pixels seems to be underestimated in comparison with the HySpex and SPOT 6/7 ones.

5 Conclusions and Perspectives

The following conclusions may be made from this study:

i. Net changes in surface elevation between December 2013 and September 2016 based on LiDAR topographic data were computed allowing to revise formal sedimentary budgets. We demonstrated that the Authie Bay is affected by a relative loss of volume between 2008 and 2016 with a sediment loss of −108,048 m^3 (−0.02 m^3/m^2) over the overall Authie estuary. Based on LiDAR data acquired between 2013 and 2016, a significant loss of volume was calculated about −219,239 m^3 (−0.04 m^3/m^2). To summarize, the sedimentary budget was highly positive between 2008 and 2011, negative between 2011 and 2013 (Crapoulet 2015) and remains negative between 2013 and 2016 (this study). The remaining question is what mechanisms control the sediment supply within the Authie Bay? It might be driven by the fact that there is less sediments inputs likely due to a decrease of the Holocene stocks in the subtidal domain or it might be a response of the spit extension which protects the inner estuary from natural sediment supply. Consequently the bay infilling might be caused by a decrease of tidal energies or currents within the estuary resulting with an increase of mud deposits along salt marshes, an infilling of the secondary channels across the salt-marches and a salt-marches prograding.

ii. In details all domains present negative sediment budgets except in the middle estuary and in the tip of the spit. However, it is well-known that the Authie bay is affected by a general infilling while locally some sites appear to be eroded between 2013 and 2016 such as the '*Bois de sapins*' site. However, it is reasonable to mention that such as analyze is relative as the morphology of the bay may drastically change with storm impacts for example. It is difficult to calculate an absolute budget at high frequency using few LiDAR data following a longer time serie. In that sense, UAV acquisitions combined to photogrammetry analysis may help to fill the gap of information.

iii. We demonstrated that is possible to map sediment bio-physical properties using both hyperspectral and multispectral data (HySpex, SPOT 6/7 and S2). We proposed to use LMM with multispectral data and MPBOM with hyperspectral data. Whatever the approach used, spatial patterns of bio-physical properties exhibited are spatially consistent with field observations and laboratory measurements and our knowledge of sedimentary processes. Whatever the sensor used, grain-size distributions and water content reveal similar patterns. Grain-size and water content are spatially highly correlated with topography. However, further investigation still needed for fully understand the role of the geomorphic structures on sediment deposits as well as the net primary production. As perspectives, grain-size maps may be used as inputs of transport models (like GSTA, 3D models, etc.) and thus for computing transport trends. Moisture content is also an important parameter to consider as the latter may be used for improving our knowledge about the cohesive behavior, the role of the Aeolian deflation over the intertidal sandy bars towards dunes in accretion for instance, etc. Finally, it is crucial to assess the distribution of microphytobenthos as the latter influence the bio-stabilization processes and thus the reworking of intertidal sediments.

iv. Regarding the biomass products, data generated from LMM may be overestimated particularly on the spit compared to MPBOM product. As a consequence, spectral algorithm choice differs from the sensor used. This may be explained by the fact that both non-linear mixing effects and scale factors are not taking into account with multispectral models.

v. Multispectral experimental models were developed with the intention to compare images each other. Developed algorithms were based on a learning dataset approach by confronting spectral behaviors directly to physical properties of the sampled sediments. Although we do not demonstrated that these algorithms are not reproducible to other coastal domains, in the frame of this study they remain useful for improving our understanding of the estuary evolution during a low tide cycle. In that sense, the synergy between various sensors presents some interesting advantages. For instance, it seems possible to predict net primary budget over time by analyzing data at various time of acquisitions. However, with the intention to determine the impact of the non-linear mixing effect on products more similar assessments are needed.

vi. To conclude, when a long time serie is available such as the multispectral S2-MSI or Landsat-OLI images, it becomes possible to better understand some processes like erosion and sandfilling interactions over time. With a high revisiting time over the same scene (5–10 days), Sentinel-2 data would be particularly well-adapted for assessing effects of seasonal variation or storm events and their respective geomorphic variations. L8 have a temporal resolution of 16 days per scene acquired. Note that Landsat serie is known to be the longest time-serie available in remote sensing starting from 1972 with Landsat-1 platform to now with Landsat-8 platform. It would be interesting to process such as data for better assessing the infilling of picard estuaries.

Acknowledgements We would like to thank the CPER-MARCO and the BQR-ULCO-TéléEST for their funding supports allowing some of the field investigations within the Bay of Authie.

Some of the image computations were performed on resources provided by the SCOSI/ULCO (Service Commun du Système d'Information de l'Université du Littoral Côte d'Opale) Infrastructure for Computing through CALCULCO platform under the TéléEST project.

This work was supported by public funds received in the framework of GEOSUD, a project (ANR-10-EQPX-20) of the program "Investissements d'Avenir" managed by the French National Research Agency which allow us to collect SPOT 6/7 images.

Hyperspectral and 2016 LiDAR data were acquired in the frame of the Défi Littoral 2016 de la Mission pour l'interdisciplinarité du CNRS. The 2013 LiDAR data were obtained through the interregional program CLAREC funded by the Regional Councils of Normandy, Picardie and Nord-Pas de Calais and by the French Centre National de la Recherche Scientifique (CNRS).

Appendice 1: Grain-Size Algorithm Used for Mapping

With the intention to derive map grain-size properties from remotely sensed data, a spectral algorithm was computed based on the matching technique between field sampling (grain-size value) and spectral information (reflectance values) for each of sampling pixels. Mean grain-size is computed such as (Eqs. 1 and 2):

$$Coarse = 215.30 * \log\left(\frac{R_{red} - R_{green}}{R_{NIR} - R_{bleue}}\right) + 290.69 \tag{1}$$

$$Fine = \left|-121.17 * \left(\frac{R_{red} - R_{green}}{R_{NIR} - R_{bleue}}\right) + 290.69\right| \tag{2}$$

where:

R_X Reflectance values for a spectral channel.

These two resulting maps (fine fraction and coarse fraction maps) were merges for obtaining a mean grain-size map. Merging criteria was defined by the following ratio (Eq. 3):

$$Ratio = \frac{R_{red} - R_{green}}{R_{NIR} - R_{red}} > X \quad (3)$$

where:

X Muddy/Sandy ratio, empirically fixed by the operator. (for this study, X range from 0.20 to 0.25).

Appendice 2: Water Content Algorithm Used for Mapping

With the intention to derive maps of water content from remotely sensed data, a spectral algorithm was computed based on laboratory measurements flowing the Verpoorter et al. (2014) approach. It consists in measuring reflectance response during dehydration process from representative sediments. Then, the resulting spectral behavior was modelled using an exponential regression function by selecting the red wavelength channel which is known for responding well to the water content changes ($R^2 = 0.77$; $P < 0.0001$). Finally, the resulting model was applied at the remotely sensed images following the Eq. (4):

$$[H_2O]\% = 87.42 * \exp^{\left(-R_{red}/0.07\right)} - 3.61 \quad (4)$$

References

Adam, S., De Backer, A., De Wever, A., Sabbe, K., Toorman, E. A., Vincx, M., et al. (2010). Biophysical characterization of sediment stability in mudflats using remote sensing: A laboratory experiment. *Continental Shelf Research*. https://doi.org/10.1016/j.csr.2009.12.008.

AQ4 Briquet, A. Le littoral du nord de la France.

Blott, S. J., & Pye, K. (2001). GRADISTAT: a grain-size distribution and statistics package for the analysis of unconsolidated sediments. *Earth Surf. Processes Landforms, 26,* 1237–1248.

Crapoulet, A. (2015). Evolution du trait de côte, bilan sédimentaire et évaluation des zones à risques sur le littoral du Nord-Pas-de-Calais: Analyse multiéchelles par LiDAR aéroporté. *These de doctorat en Geographie Physique. Wimereux: Universite du Littoral Cote d'Opale*.

Combe, J. P., Launeau, P., Carrere, V., Despan, D., Meleder, V., Barillé, L., et al. (2005). Mapping microphytobenthos biomass by non-linear inversion of visible-infrared hyperspectral images. *Remote Sensing of Environment, 98,* 371–387. https://doi.org/10.1016/j.rse.2005.07.010.

Deloffre, J., Verney, R., Lafite, R., Lesueur, P., Lesourd, S., & Cundy, A. B. (2007). Sedimentation on intertidal mudflats in the lower part of macrotidal estuaries: Sedimentation rhythms and their preservation. *Marine Geology, 241,* 19–32. https://doi.org/10.1016/j.margeo.2007.02.011.

Deronde, B., Houthuys, R., Henriet, J.-P., & Lancker, V. V. (2008). Monitoring of the sediment dynamics along a sandy shoreline by means of airborne hyperspectral remote sensing and LIDAR:

A case study in Belgium. *Earth Surface Processes Landforms, 33,* 280–294. https://doi.org/10.1002/esp.1545.

Dobroniak, C. (2005). Morphological evolution and management proposals in the Authie Estuary, northern France. *Proceeding Dunes and Estuaries, 2205,* 537–545.

Folk, R. L., & Ward, W. C. (1957). Brazos river bar: A study in the significance of grain-size parameters. *Journal of Sedimentary Petrology, 27,* 3–26.

Green, A. A., Berman, M., Switzer, P., & Craig, M. D. (1988). A transformation for ordering multispectral data in terms of images quality with implications for noise removal. *IEEE Transactions on Geoscience and Remote Sensing, 26*(1), 65–74.

Hagolle, O., Huc, M., Villa Pascual, D., & Dedieu, G. (2010). A multi-temporal method for cloud detection, applied to FORMOSAT-2, VENµS, LANDSAT and SENTINEL-2 images. *Remote Sensing of Environment, 114*(8), 1747–1755.

Hesp, P. A., Ruz, M.-H., Hequette, A., Marin, D., & Miot da Silva, G. (2016). Geomorphology and synamics of a travelling cuspate foreland, Authie estuary France. *Geomorphology, 254,* 104–120. https://doi.org/10.1016/j.geomorph.2015.11.015.

Kazemipour, F., Launeau, P., & Méléder, V. (2012). Microphytobenthos biomass mapping using the optical model of diatom biofilms: Application to hyperspectral images of Bourgneuf Bay. *Remote Sensing of Environment, 127,* 1–13.

Launeau, P., Méléder V., Verpoorter, C., Barillé, L. Kazemipour F., Giraud, M., et al. (2018). Microphytobenthos biomass and diversity mapping at different spatial scales with hyperspectral optical model. *Remote Sensing, 10*(5), 716.

Laben, C. A., & Bower, B. V. (2000). Process for enhancing the spatial resolution of multispectral imagery using pan-sharpening. US Patent 6.011875.

AQ5 Latteux, B. (2001). *Synthèse sur les problématiques et enjeux d'évolution du littoral haut-normand et picard-1*. DDE de la somme: Milieu Physique.

Rainey, M. P., Tyler, A. N., Gilvear, D. J., Bryant, R. G., & McDonald, P. (2003). Mapping intertidal estuarine sediment grain size distributions through airborne remote sensing. *Remote Sensing of Environment, 86,* 480–490. https://doi.org/10.1016/S0034-4257(03)00126-3.

Méléder, V., Launeau, P., Barillé, L., Combe, J. P., Carrère, V., Jesus, B., et al. (2010). Hyperspectral imaging for mapping microphytobenthos in coastal areas. In M. Maanan & M. Robin (Eds.), *Geomatic solutions for coastal environments* (pp. 71–139). New York: Nova Science Publishers Inc.

Small, C., Steckler, M., Seeber, L., Akhter, S. H., Goodbred, S., Jr., Mia, B., et al. (2009). Spectroscopy of sediments in the Ganges-Brahmaputra delta: Spectral effects of moisture, grain size and lithology. *Remote Sensing of Environment, 113,* 342–361. https://doi.org/10.1016/j.rse.2008.10.009.

Smith, G. M., Thomson, A. G., Moller, I., & Krompkamp, J. C. (2004). Using hyperspectral imaging for the assessment of mudflat surface stability. *Journal of Coastal Research*, *20*(4), 1165–1175. West Palm Beach (Florida). ISSN 0749-0208.

Sogreah, (2009). Diagnostic, étude d'opportunité et de faisabilité pour l'aménagement de la rive Nord de l'Authie. *Rapport provisoire. Communauté de Communes Opale Sud.*

Tucker, C. J. (1979). Red and photographic infrared linear combinations for monitoring vegetation. *Remote Sensing of Environment, 8,* 127–150. https://doi.org/10.1016/0034-4257(79)90013-0.

Ubertini, M., Lefebvre, S., Gangnery, A., Grangeré, K., Gendre, R. L., & Orvain, F. (2012). Spatial variability of benthic-pelagic coupling in an estuary ecosystem: Consequences for microphytobenthos resuspension phenomenon. *PLoS ONE, 7,* e44155.

Verpoorter, C., Carrère, V., & Combe, J. P. (2014). Visible, near-infrared spectrometry for simultaneous assessment of geophysical sediment properties (water and grain size) using the Spectral Derivative–Modified Gaussian Model. *Journal of Geophysical Research : Earth Surface, 119*, 2098–2122. hal- 01130379.

Author Queries

Chapter 45

Query Refs.	Details Required	Author's response
AQ1	Please check and confirm if the authors and their respective affiliations have been correctly identified. Amend if necessary.	
AQ2	Reference 'Briquet et al. (1930)' is cited in the text but not provided in the reference list. Please provide the respective reference in the list or delete this citation.	
AQ3	Kindly note that the reference 'Laben et al. (2000), Tucker et al. (1979), Crapoulet et al. (2015),Rainey et al. (2006), Deloffre et al. (2017) and Small et al. (2012) ' have been changed to 'Laben and Bower (2000), Tucker (1979), Crapoulet (2015), Rainey et al. (2003), Deloffre et al. (2007) and Small et al. (2009)' so that this citation matches the list.	
AQ4	Please provide full Details for Reference 'Briquet, A. Le littoral du nord de la France'.	
AQ5	References 'Latteux (2001), Smith et al. (2004), Ubertini et al. (2012)' are given in the list but not cited in the text. Please cite them in text or delete them from the list.	

MARKED PROOF

Please correct and return this set

Please use the proof correction marks shown below for all alterations and corrections. If you wish to return your proof by fax you should ensure that all amendments are written clearly in dark ink and are made well within the page margins.

Instruction to printer	*Textual mark*	*Marginal mark*
Leave unchanged	· · · under matter to remain	
Insert in text the matter indicated in the margin		New matter followed by or
Delete	/ through single character, rule or underline or through all characters to be deleted	or
Substitute character or substitute part of one or more word(s)	/ through letter or through characters	new character / or new characters /
Change to italics	under matter to be changed	
Change to capitals	under matter to be changed	
Change to small capitals	under matter to be changed	
Change to bold type	under matter to be changed	
Change to bold italic	under matter to be changed	
Change to lower case	Encircle matter to be changed	
Change italic to upright type	(As above)	
Change bold to non-bold type	(As above)	
Insert 'superior' character	/ through character or where required	or under character e.g. or
Insert 'inferior' character	(As above)	over character e.g.
Insert full stop	(As above)	
Insert comma	(As above)	,
Insert single quotation marks	(As above)	or and/or or
Insert double quotation marks	(As above)	or and/or or
Insert hyphen	(As above)	
Start new paragraph		
No new paragraph		
Transpose		
Close up	linking characters	
Insert or substitute space between characters or words	/ through character or where required	
Reduce space between characters or words	between characters or words affected	